Adult Stem Cell Subsets from Adult Human Dermis

Journal of
Stem Cell Research & Therapy
ISSN: 2157-7633

Vega-Crespo et al., J Stem Cell Res Ther 2018, 8:2
DOI: 10.4172/2157-7633.1000411

Research Article Open Access

Adult Stem Cell Subsets from Human Dermis

Agustin Vega-Crespo[1,2*], Brian Truong[1,2], Benjamen E. Schoenberg[1,2], Alexandra K. Ciminera[1,2], Benjamin L. Larson[3,4,5,6], Daniel G. Anderson[3,4,5,6,7] and James Byrne[1,2]

[1]*Department of Molecular and Medical Pharmacology, University of California, USA*
[2]*Eli and Edythe Broad Center of Regenerative Medicine and Stem Cell Research, University of California, USA*
[3]*Department of Chemical Engineering, Massachusetts Institute of Technology, USA*
[4]*David H. Koch Institute for Integrative Cancer Research, Massachusetts Institute of Technology, USA*
[5]*Department of Anesthesiology, Boston Children's Hospital, USA*
[6]*Harvard-MIT Division of Health Sciences and Technology, Massachusetts Institute of Technology, USA*
[7]*Institute for Medical Engineering and Science, Massachusetts Institute of Technology, USA*

Abstract

Adult stem cells possess the ability to differentiate and mature into defined cell types; however, tissue-specificity and donor and culture inconsistencies have presented a challenge in identifying these cells. Adult adherent dermal cell-products have been efficiently utilized for isogenic cosmetic therapies. The purpose of this study is to identify, isolate, and characterize progenitor subsets from adult adherent dermal cells capable of *ex vivo* differentiation. LAVIV® adult dermal cells were independently immunoselected for CD146, CD271, and CD73/CD90/CD105 to investigate the mesenchymal differentiation capacity and possible enrichment in the purified fractions. After differentiation, the osteogenic, chondrogenic, and adipogenic potential and cell-specific gene expression were evaluated and compared for each phenotype. Adult dermal cells possess the ability to differentiate into the three cell lineages, osteocyte, chondrocyte, and adipocyte that co-express the adult stem cell immunophenotypic markers CD146 and CD271 with independent enrichment of the multipotent capacity for both fractions. We conclude that subpopulations in human dermal primary cultures possess the potential to differentiate into other cell types providing a novel source of multipotent cells for regenerative medicine.

Keywords: Adult stem cells; Cosmetic therapies; Osteocyte; Chondrocyte; Adipocyte; Regenerative medicine

Introduction

Human adult mesenchymal stem cells (hMSC) possess the ability to adhere to common tissue culture-treated plastic, expand *in vitro* into a clinically relevant number of cells, and differentiate into a variety of cell types including osteoblasts, chondrocytes, and adipocytes [1,2]. This multi-lineage capacity differs among niches, conditions, and duration of *in vitro* culture [3-7]. The hMSC cell surface signature enables the ability to identify and isolate certain stromal-like cell derivatives, which can undergo *ex vivo* differentiation resulting in committed cell lineages [1,8]. The cellular surface markers reported in literature that may be accompanying an augment to the *in vitro* differentiation potential is certainly large, however, this potential varies drastically among tissues and in certain instances, the surface signature does not correlate with the *in vitro* degree of phenotype functionality [9]. Among these cellular surface markers, the canonical surface markers 5'-nucleotidase, ecto (CD73) or NT5E, thymocyte antigen 1 (CD90) or Thy-1 and Endoglin (CD105), were initially described as unique for mesenchymal stromal cells, but have since been identified as distributed among diverse types of human cells including fibroblasts with some or no *in vitro* mutipotency [1,8]. Previous research in human adult adipose cells and human neonatal dermal derivatives suggest Melanoma Cell Adhesion Molecule (CD146) or MCAM [10] and nerve growth factor receptor (CD271) or NGFR [11], respectively, as putative candidate markers to isolate mesenchymal stromal-like cells from human adult dermal derivatives, which would enhance the ability of forming bone, cartilage, and fat *ex vivo*. In theory, adult multipotent dermal fibroblasts can be easily attained through a minimally invasive and relatively painless skin punch biopsy [12] and hMSC derivatives purified via cell surface markers for *in vitro* or *in vivo* clinical applications [9,13]. The purpose of our study includes the identification and isolation of progenitor subsets from adult dermis and characterization of the *in vitro* multipotent potential associated with a specific phenotype.

Material and Methods

In vitro culture of primary human skin cells

LAVIV® (azficel-T by Fibrocell Science, DR01) adult human skin-derived dermal fibroblast utilized in this study were obtained from a 4 mm skin punch biopsy as described on Isolagen Standardized Manufacturing Process EX-GTR-110 Version Number 00. All human biopsy-derived cells were cultured in regular cell culture media consisting of Dulbecco's modified Eagle medium nutrient mixture DMEM/F-12 (Life Technologies, 11320-082) supplemented with 10% fetal bovine serum (Life Technologies, 26140-079), 1% MEM nonessential amino acids (Life Technologies, 11140-076), 2 mM GlutaMAX (Life Technologies, 35050-061), and Primocin 100 µg/mL (Invivogen, ant-pm-1). The culture media was changed every 2 days. The cells were allowed to expand to >90% confluency before passaging with 0.05% trypsin-EDTA (Gemini Bio-Products, 400-150) and replating at 8,400 cells/cm^2 [13-15].

Live cell staining and fluorescence activated cell sorting-based purification

Approximately 1 × 10^7 cells were trypsinized and washed twice with

***Corresponding author:** Agustin Vega-Crespo, Department of Molecular and Medical Pharmacology, University of California, Los Angeles, 650 Charles E. Young Drive South, 23-120 Center for Health Sciences, Los Angeles, CA 90095, USA, Tel: 714-469-6836; E-mail: avegacrespo@mednet.ucla.edu

Received January 22, 2018; **Accepted** February 06, 2018; **Published** February 28, 2018

Citation: Vega-Crespo A, Truong B, Schoenberg BE,Ciminera AK, Larson BL, et al. (2018) Adult Stem Cell Subsets from Human Dermis. J Stem Cell Res Ther 8: 411. doi: 10.4172/2157-7633.1000411

ice-cold phosphate-buffered saline (PBS) + 2% goat serum (Gemini Bio-Products, 100-109) (PBS-G). The cells were then passed through a 40 μm filter to remove clumps and resuspended as 4-5 × 10^6 cells in 0.1 mL of ice-cold PBS-G containing: [A] 1:100 CD146:FITC antibody (AbD Serotec, MCA2141F) [16], [B] 1:200 CD271:AlexaFluor 647 (BD Bioscience, 560326) [11], and [C] 1:100 CD73:PE-Cy7 (BD Bioscience, 561258), CD90:PE antibody (BD Bioscience, 555596), and CD105: AlexaFluor 647 antibody (BD Bioscience, 561439) [17]. Samples were incubated for 30 min in the dark at 4°C with gentle nutation. The cells were washed thrice with ice-cold PBS-G, resuspended in 1 mL of ice-cold PBS-G, passed through a 40 μm filter, and immediately analyzed and sorted on a FACSAria cell sorter (BD Biosciences). Data were analyzed; DAPI-stained (Life Technologies, D1306) dead-cell exclusion and doublet-exclusion gating were performed; and viable single-cell subpopulations were sorted using BD FACSDiva Software (BD Biosciences) [9]. Positive and negative purified fractions alongside a mix-whole sort sample were allowed to recover and expanded for 1-week before a second round of FACS-purification.

Osteogenic-differentiation

LAVIV® adult human skin-derived dermal cells were plated at 4,400 cells/cm^2 [25] and allowed to expand to >90% confluency before the commencement of the hMSC-differentiation protocol (Lonza, PT-3002). hMSC differentiation basal medium consisted of Dulbecco's Modified Eagle medium nutrient mixture-low glucose supplemented with 10% heat inactivated MSC-fetal bovine serum, 2 mM L-Glutamine and Primocin 100 μg/mL. The complete hMSC differentiation osteogenic medium was comprised of hMSC differentiation basal medium and freshly added 0.1 μM dexamethasone, 0.2 mM ascorbic acid 2-phospate and 10 mM glycerol 2-phosphate. Medium was supplemented every 72-hours [18,19].

Adipogenic-differentiation

LAVIV® adult human skin-derived dermal cells were plated at 4,400 cells/cm^2 and allowed to expand to >90% confluency before the commencement of the hMSC-differentiation protocol (Lonza, PT-3004). hMSC differentiation basal medium consisted of Dulbecco's Modified Eagle medium nutrient mixture supplemented with 10% heat inactivated MSC-fetal bovine serum, 2 mM L-Glutamine and Primocin 100 μg/mL. The complete hMSC differentiation adipogenic medium was hMSC differentiation basal medium and freshly added 1 μM insulin (human recombinant), 1 μM dexamethasone, 0.2 mM indomethacin, 0.1875 mM IBMX (3-isobutyl-l-methyl-xanthine). Medium was supplemented every 72-hours [18,19].

Chondrogenic-differentiation

LAVIV® adult human skin-derived dermal cells were plated at 8,800 cells/cm^2 and allowed to expand to >90% confluency before the commencement of the hMSC-differentiation protocol (Lonza, PT-3003) [30] supplemented with TGF-B3 (Lonza, PT-4124) [31]. Chondrogenic-hMSC differentiation basal medium consisted of Dulbecco's Modified Eagle medium nutrient mixture supplemented with 2 mM L-Glutamine, 100 μg/mL sodium pyruvate, 40 μg/mL proline, ITS+supplement (6.25 μg/mL human recombinant insulin, 6.25 μg/mL transferrin, 6.25 μg/mL selenous acid, 5.33 μg/mL linoleic acid, and 1.25 mg/mL bovine serum albumin), 50 μg/mL ascorbate, 100 nM dexamethasone, and Primocin 100 μg/ml [32]. The complete hMSC differentiation chondrogenic medium was comprised of Chondrogenic-hMSC differentiation basal medium and freshly added TGF-B3 at a final concentration of 10 ng/mL [20]. Chondrogenic pellets were formed according to the manufacturer's recommendations and medium was supplemented every 72-hours [19,20].

In Vitro Analysis

Alizarin red S

At day 21 of osteogenic induction, the level of mineral deposition was inspected using Alizarin Red S [40 mM] pH 4.1-4.5 (Sigma, A5533). Alizarin Red Staining and the quantitative analysis of Alizarin Red staining were executed according to manufacturer recommendations (Millipore, ECM815) [21]. Light microscopy-based imaging was performed with an AxioCam HR Color Camera using AxioVision Digital Image Processing Software (Axio Observer Inverted Microscope, Carl Zeiss). Alizarin Red colorimetric determinations were performed at OD405 pH 4.1-4.5 in 96-well format (Costar, 07-200-568) using the Tecan Infinite 200 multimode microplate reader provided with Tecan-i-Control Plate reader Analysis Software (Tecan).

Oil Red and adipored assay

At day 21 of adipogenic induction, lipid droplet accumulation was inspected utilizing 5 mg/mL Oil Red O (Sigma, O0625) in isopropyl alcohol and distilled water [22]. After a 10-minute incubation, light microscopy-based imaging was performed with an AxioCam HR Color Camera using AxioVision Digital Image Processing Software (Axio Observer Inverted Microscope, Carl Zeiss). The AdipoRed Assay (Lonza, PT-7009) was applied to quantitatively determine the lipid content. Fluorescence was measured with excitation at 485 nm and emission at 572 nm as per manufacturer recommendations [23]. All readings were executed in 24-well format (Costar, 07-200-84) using the Tecan Infinite 200 multimode microplate reader provided with Tecan-i-Control Plate reader Analysis Software (Tecan).

Toluidine blue O

At day 21 of chondrogenic induction, chondrogenic pellets were fixed in 4% PFA, embedded with OCT and 5 μm sections were obtained [24]. The production of proteoglycan constituents and chondromucin aggregates were evaluated utilizing an acid solution of 1 mg/mL Toluidine Blue O (Sigma, 198161) pH 2.0-2.5 in 70% alcohol and distilled water [25]. After a 3-minute incubation, light microscopy-based imaging was performed with an AxioCam HR Color Camera using AxioVision Digital Image Processing Software (Axio Observer Inverted Microscope, Carl Zeiss).

Quantitative reverse transcription-polymerase chain reaction

Total RNA was isolated from cultures with a Roche High Pure RNA Isolation Kit (Roche Applied Sciences, 011828665001) and 10 ng^{-1} μg were reverse transcribed to cDNA utilizing a Transcriptor First Strand cDNA Synthesis Kit (Roche Applied Sciences, 04379012001) following the manufacturer's instructions. Primers and probes were designed from Roche's Universal Probe Library. Primers for the genes were synthesized at Valuegene Inc. and listed on (Table 1). Quantitative PCR relative expression experiments were performed on a LightCycler 480 Real-Time PCR System (Roche), and data were further analyzed with LightCycler 480 Software release 1.5.0. with 1-10 ng of sample in a total of 20 μL of reaction mix consisting of 10 μM UPL probe, 20 μM of forward and reverse primers and 2X-LightCycler 480 Probes Master Mix. Triplicate experimental samples were paired using the all-to-mean pairing rule, ΔΔCt value calculation with three housekeeping genes run in triplicate for advanced relative quantification [14,26].

Gene	GenBank ID	Length	Primer Sequence	Probe	Amplicon
ACTB	NM_001101.3	1852	F: 5' CCAACCGCGAGAAGATGA 3' R: 5' CCAGAGGCGTACAGGGATAG 3'	64	97
AGC-1	L12234	114	F: 5' TGCCATCGACTCTTTCACAT 3' R: 5' AATCTCACACAGGTCCCCTTC 3'	33	61
BMP-2	NM_001200.2	7770	F: 5' CAGACCACCGGTTGGAGA 3' R: 5' CCCACTCGTTTCTGGTAGTTCT 3'	71	95
CBFA-1	AF053952.1	296	F: 5' GGTTAATCTCCGCAGGTCAC 3' R: 5' GTAAATACTGCTTGCAGCCTTAAAT 3'	83	106
CEBPA	NM_004364.3	2591	F: 5' AGTTCCTGGCCGACCTGT 3' R: 5' CCCGGGTAGTCAAAGTCG 3'	74	103
COL-2A1	ENSG00000139219.12	546	F: 5' AGGGCCAGGATGTCCATT 3' R: 5' AGGAGAGGGCCCACAGAG 3'	13	97
COMP	ENSG00000105664.4	585	F: 5' AGAAGAGCAACCCGGATCA 3' R: 5' CCCGAGAGTCCTGATGTCC 3'	58	102
FABP-4	ENSG00000170323.4	941	F: 5' CCACCATAAAGAGAAAACGAGAG 3' R: 5' GTGGAAGTGACGCCTTTCAT 3'	31	70
GAPDH	ENST00000229239.5	1875	F: 5' GCTCTCTGCTCCTCCTGTTC 3' R: 5' ACGACCAAATCCGTTGACTC 3'	60	115
HPRT-1	ENST00000298556.7	1407	F: 5' TGACCTTGATTTATTTTGCATACC 3' R: 5' CGAGCAAGACGTTCAGTCCT 3'	73	102
OC	X53698.1	451	F: 5' GGCGCTACCTGTATCAATGG 3' R: 5' TCAGCCAACTCGTCACAGTC 3'	79	106
OP	J04765.1	1447	F: 5' TTTCGCAGACCTGACATCC 3' R: 5' GGCTGTCCCAATCAGAAGG 3'	61	139
PPARG-2	NM_015869.4	1820	F: 5' GACAGGAAAGACAACAGACAAATC 3' R: 5' GGGGTGATGTGTTTGAACTTG 3'	7	96
VCAN-1	NM_004385.4	12416	F: 5' TGTATTGTTATGTGGATCATCTGGA 3' R: 5' CTGGAGTTCCCCCACTGTT 3'	64	131

Table 1: List of primers: forward primer (F) and reverse primer (R) used for amplification using qPCR of β-actin (ACTB), aggrecan, exon 1 (AGC-1), bone morphogenetic protein 2 (BMP-2), core-binding factor alpha subunit 1 (CBFA-1), runt-related transcription factor 2 (RUNX-2), CCAAT/enhancer binding protein alpha (CEBPA), collagen type II alpha 1 (COL-2A1), cartilage oligomeric matrix protein (COMP), fatty acid binding protein 4, adipocyte (FABP-4), glyceraldehyde 3-phosphate dehydrogenase (GAPDH), hypoxanthine phosphoribosyltransferase 1 (HPRT-1), osteocalcin (OC), osteopontin (OP), peroxisome proliferator-activated receptor gamma variant 2 (PPARG2) and versican (VCAN-1) genes. Universal probe library (UPL) number, target region length (GenBank ID number) and amplicon size in base pairs (bp) are cited for reference.

Statistical analysis

All collected data were coded and analyzed with the SPSS statistical package (21.0 Version). Results are expressed as mean, Standard Deviation (SD) with a confidence interval of 95%. The Levene test for equality of variances was used to analyze the normal distribution of the variables ($p>0.05$). Quantitative data without a normal distribution were analyzed with non-parametric tests (Mann–Whitney U and Kolmogorov-Smirnov), and data with a normal distribution were analyzed with parametric tests as for independent sample t test and 2-way analysis of variance (ANOVA). Bonferroni and Dunnet T3 test were performed for post-hoc analyses. A P value less than 0.05 was considered statistically significant. All graphs were generated utilizing GraphPad Prism 6 [27,28].

Results

Identification of mesenchymal-like cells in human dermis

Adult human dermal biopsies contain a variety of cells with discrete multipotent phenotypes [3-11], which are lost over extended culture periods [5]. The presence or absence of certain markers (CD73, CD90, CD105, CD146, CD271) associated with *ex vivo* multipotency appears to depend on factors such as biopsy procedure and expansion, cell density, culture conditions, and longevity of culture [5,9,10]. LAVIV® azficel-T cells contained 3% dermal derivatives expressing CD271 and 20% expressing CD146; positive and negative fractions for both phenotypes were independently collected. CD73, CD90, and CD105 were expressed at >95%; the High-30% expressing triple positive and its counterpart Low-30% were collected alongside a mix-whole sort and utilized as an experimental control. Following one week of culture, the CD271+ FACS-purified fraction dramatically decreased to 8% and CD146+ fraction to 79% (Figure 1A). As for CD73, CD90, and CD105, both fractions High-30 and Low-30% remained unaffected with serial sorting (Figure 1B).

In vitro osteogenic profile

LAVIV® adult human skin-derived dermal fractions undergoing osteogenic differentiation contain cells with and without the ability to differentiate into osteoblasts. Independent phenotype enrichment separates these distinct cell populations. The CD146+ cells appeared not to co-express CD271+ on a multicolor flow cytometry plot (data not shown). The high expression of the canonical mesenchymal markers CD73, CD90 and CD105 (triple positive fraction) appeared to co-express distinctly with CD146 and CD271 (data not shown), however, we did not analyze the independent correlation and co-expression between CD146 and CD271 with the high and low fractions of these triple positive cells. The osteogenic potential of the adherent cells was assessed qualitatively (Figure 2A) and quantitatively (Figure 2B) by Alizarin Red Staining [ARS]. Measurements were calibrated over a Non-differentiated Control [ND] that consisted of Mix-Whole Sort-cells (WS) that underwent the differentiation protocol with only basal media (no differentiation factors). Differentiated cultures were stained by ARS, and osteogenic differentiation was evaluated by the amount of red staining (black arrows Figure 2A) on the mineral-rich extracellular pockets secreted by osteoblast-like cells. This visual assessment revealed an osteogenic enrichment for CD146+, CD271+, and High-30% phenotype over their negative phenotype counterparts and WS. Figure 2B quantitatively corroborated the findings that CD146-expressing cells resulted in a statistically significant osteogenic enrichment above the other phenotypes followed by CD271-expressing

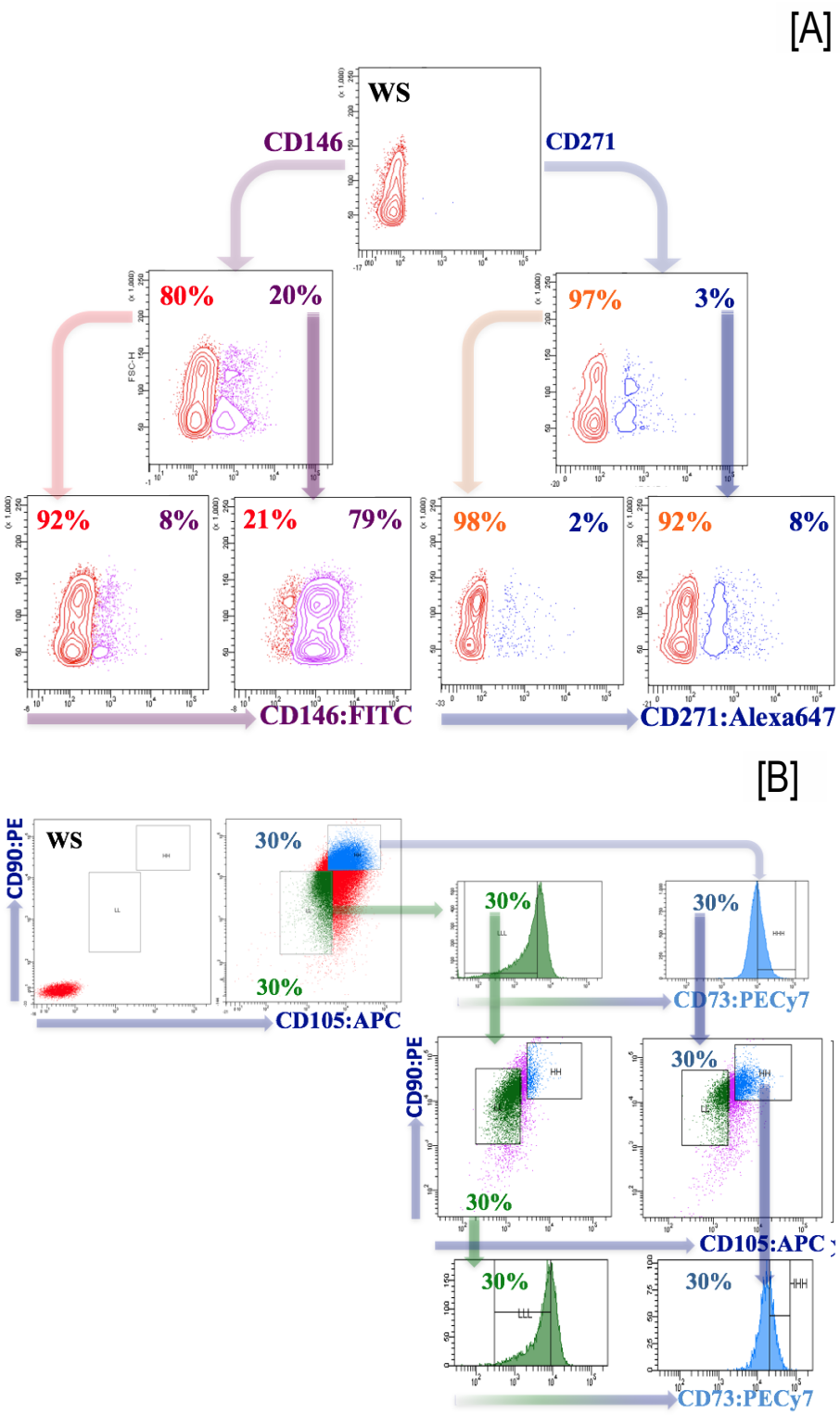

Figure 1: Analysis of LAVIV® azficel-T dermal cells by flow cytometry and FACS based purification plots. FACS Aria cell sorter was pre-adjusted and calibrated to very high purity for all purifications. [A] CD146 (left arm) double purification path: CD146+ phenotype lost >20% of expression whereas 8% of the negative phenotype appeared positive post- 1X SORT. CD271 (right arm) double purification path: CD271+ phenotype lost >90% of expression whereas 2% of the negative phenotype appeared positive post- 1X SORT. [B] CD73, CD90 and CD105 were expressed at >95%; the High-30% expressing triple positive and its counterpart Low-30% maintained unaltered post- 1X SORT. All of the 7-fractions of dermal derivatives: Mix-whole sort [WS], CD146+, CD146-, CD271+, CD271-, High-30% and Low-30% were collected post- 2X SORT and immediately plated for further in vitro differentiation into bone, fat and cartilage.

cells. High-30%-Expressing triple positive cells were more osteogenic than Low-30% but not more osteogenic than WS.

Results were confirmed by qPCR (Figure 2C) evaluating the relative gene expression (RGE) for osteoblastic extracellular matrix components: Osteocalcin [OC], a non-collagenous protein secreted solely by osteoblasts that controls osteoblast maturation or "bone-building" by regulating bone mineralization and calcium homeostasis, and Osteopontin [OP], a linking- extracellular structural protein that actively participates in bone remodeling and bone bio-mineralization by binding to various types of calcium-base biomaterials. Ostoegenic commitment was scrutinized by quantification of the transcript levels of runt-related transcription factor 2 [RUNX-2] and CCAAT/enhancer Binding Protein Alpha [CBFA-1], pivotal kinase-dependent regulators of the osteoblast phenotype with the ability to re-direct committed cells into an osteoblast lineage and to directly stimulate downstream osteoblast-specific genes. These include OC, OP, bone sialoprotein, and alkaline phosphatase. An additional factor monitored included bone morphogenetic protein-2 [BMP-2], which induces differentiation of multipotent cells to an osteoblast lineage and promotes bone formation by triggering the transcription of early osteogenic lineage-specific factors such as distal-less homeobox-5 [DLX5] and CBFA-1 [29,30]. Figure 2C showed OC RGEs were significantly greater for CD146+, CD271+, and High-30% than the negative phenotypes and WS. When comparing OP RGE in CD146+ and CD271+ fractions to the rest of the fractions, the High-30% phenotype was no different than Low-30% and WS. CBFA-1 RGE was significantly greater for CD146+, CD271+, and High-30% than the negative phenotypes and WS. When comparing BMP-2 RGE in CD146+ and CD271+ fractions to the rest of the fractions, the High-30% phenotype was no different than Low-30% and WS. In summary, CD146+, CD271+, and High-30% phenotypes may independently enrich for osteogenic cells from adult human dermis. Under our culture system and given experimental parameters, CD146- expressing dermal derivatives were more apt to form bone *in vitro*.

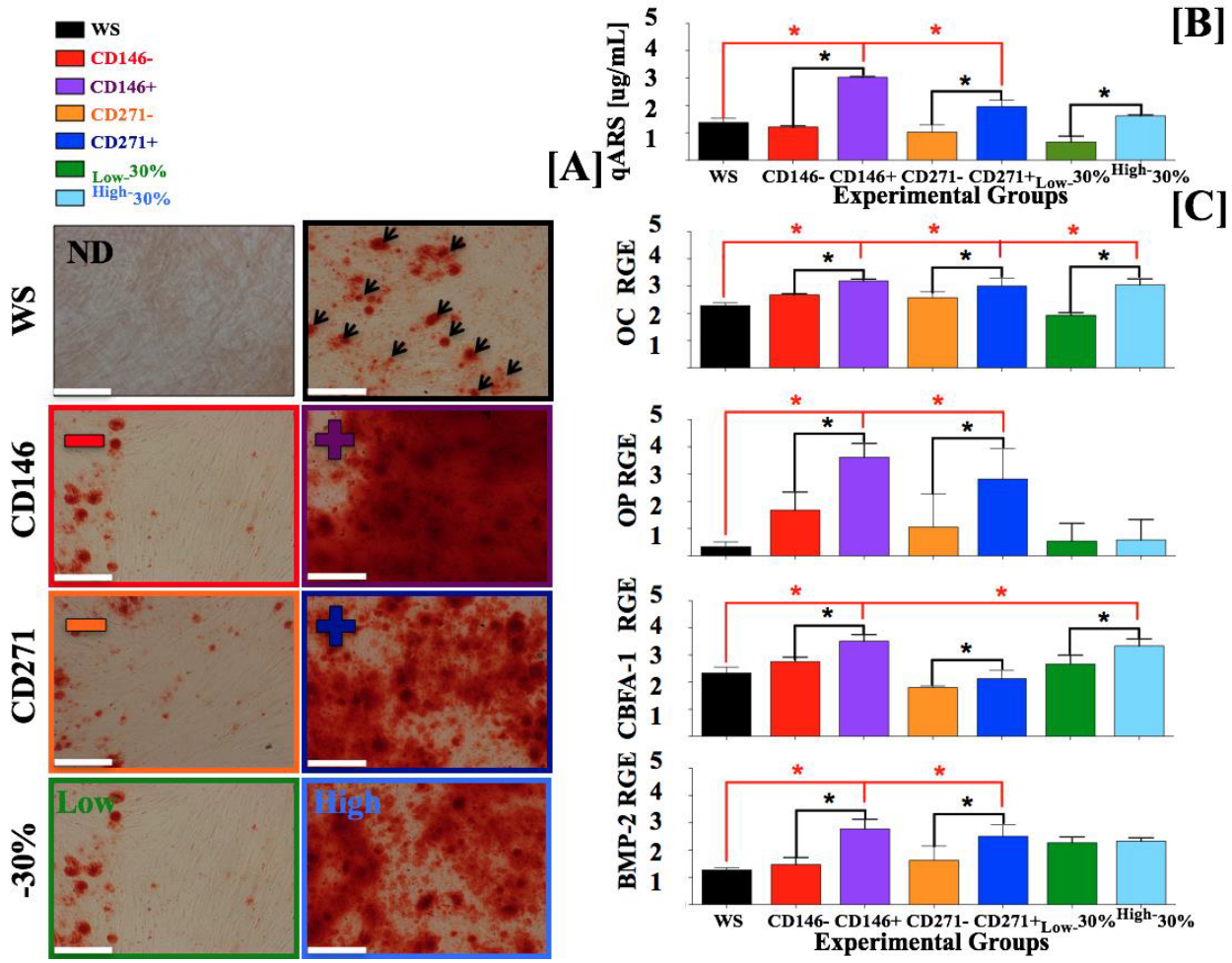

Figure 2: **[A]** Adherent dermal cells after osteogenic differentiation stained for Alizarin red where: **WS** = Mix-whole sort, **ND** = Mix-whole sort **N**ot-**D**ifferentiated control, **Arrowheads** (upper right photomicrograph) indicate osteogenic pockets, **Black** = WS, **Red** = CD146+, **Purple** = CD146-, **Orange** = CD271+, **Blue** = CD271-, **Green** = $_{Low-}$30%, **Azure** = $^{High-}$30%. Bar = 200 µm. **[B]** Quantitative Alizarin red extraction of adherent dermal cells after osteogenic differentiation measured on uptake of Alizarin red in µg/mL (*y* axis) among experimental groups (*x* axis). Error bars indicate mean ± standard deviation **[SD]** (*n*=6). **Black** indicates significance *p<0.05 between positive/= $^{High-}$30% vs. negative/ $_{Low-}$30%. **Red** indicates significance *p<0.05 against WS. **[C]** Quantitative real time PCR **[qPCR]** of adherent dermal cells after osteogenic differentiation measured in **R**elative **G**ene **E**xpression (*y* axis) among experimental groups (*x* axis). Error bars indicate mean ± standard deviation **[SD]** (*n*=3). **Black** indicates significance *p<0.05 between positive/= $^{High-}$30% vs. negative/ $_{Low-}$30%. **Red** indicates significance *p<0.05 against WS.

Although CD271+ and High-30% enhanced bone formation in our cultures, the data was not as robust.

In vitro chondrogenic profile

LAVIV® adult human skin-derived dermal fractions underwent chondrogenic differentiation into glycoprotein-secreting chondrocytes with a modest enrichment of the CD271+ and CD146+ phenotypes. Qualitative Toluidine blue O [TBO] staining was performed. The blue dye specifically formed complexes with Anionic Glycoconjugates (AG) such as Proteoglycans (PG) and Glicosaminoglycans (GAG), which are produced by chondrocyte-like cells (Figure 3A).

To confirm the chondrogenic potential of dermal fractions, a qPCR-evaluation was performed from culture replicates for extracellular cartilage-forming proteins including:

- Cartilage Oligomeric Matrix Protein [COMP], a non-collagenous flexible "lattice" protein that maintains cell-to-cell organization and binding interactions,
- Versican [VCAN-1], a chondroitin sulfate proteoglycan with numerous non-structural functions in cartilage-like tissue, such as chondrocyte proliferation [50],
- Collagen, type II, alpha 1 [COL2A01], the primary structural protein in cartilage, located almost exclusively in cartilage, and
- Aggrecan [AGC-1], a cartilage-specific proteoglycan core protein that provides gel-structure and cartilage load-bearing capabilities [1,31,32].

In addition, we also examined the RGE for BMP-2; although the molecular mechanism is still unclear, BMP-2 has been reported to initiate, promote and maintain the chondrogenic phenotype in high-density cultures [33]. Figure 3B showed COMP and VCAN-1 RGE patterns are greater for CD146+, CD271+ and High-30% fractions than the negative phenotypes and WS. COL2A-1, AGC-1, and BMP-2 RGEs were also similar for CD146+ and CD271+ compared to all other fractions; High-30% phenotype was no different than Low-30% and WS. Whereas TBO uptake was qualitatively observed to be higher for CD146+ cells, 3 of the 5 genes studied were statistically higher in the CD271+ phenotype than in the CD146+ phenotype (Mann–Whitney

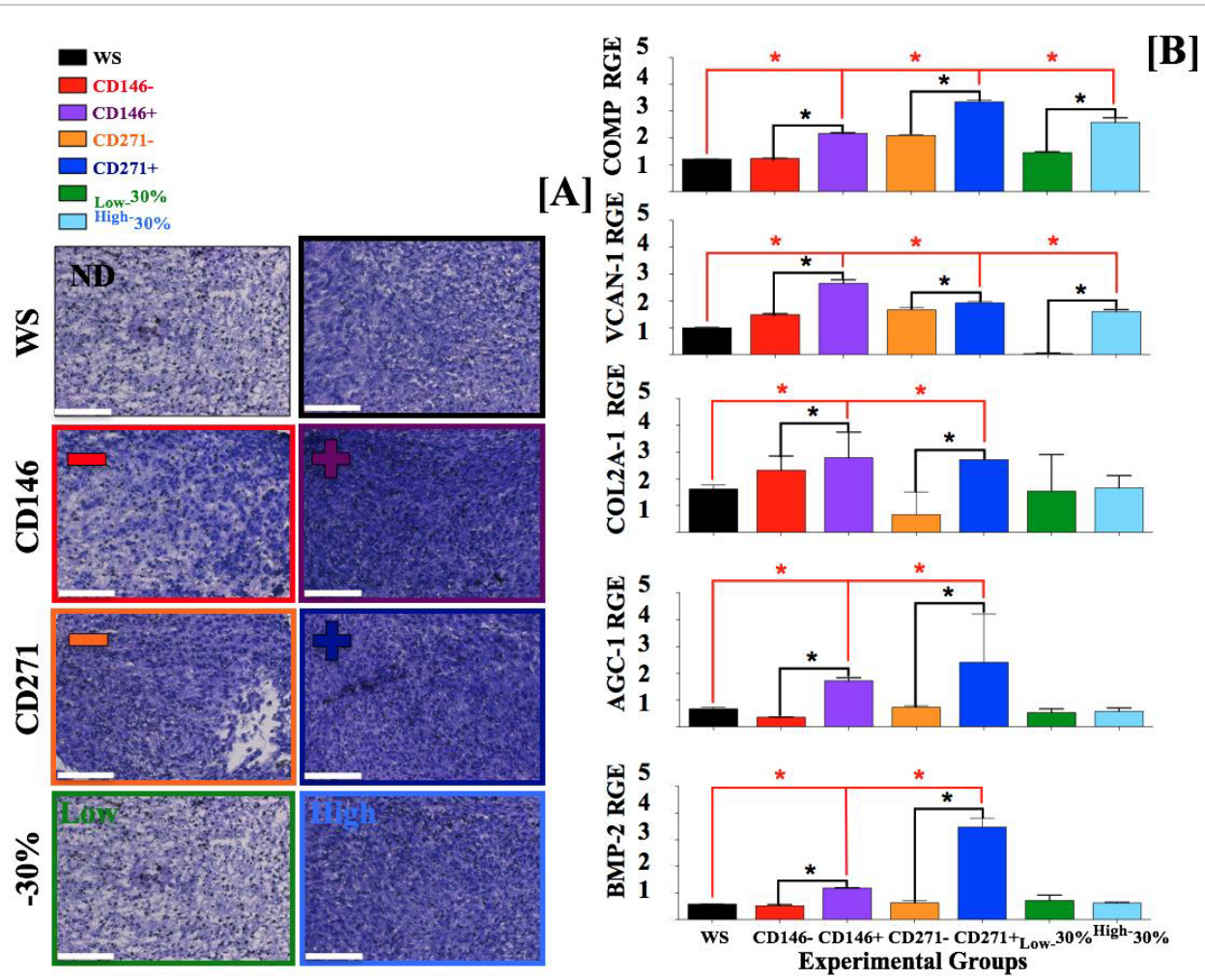

Figure 3: **[A]** Adherent dermal cells after chondrogenic differentiation stained for Toluidine Blue O where: **WS** = Mix-whole sort, **ND** = Mix-whole sort **N**ot-**D**ifferentiated control, **Black** = WS, **Red** = CD146+, **Purple** = CD146-, **Orange** = CD271+, **Blue** = CD271-, **Green** = $_{Low-}$30%, **Azure** = $^{High-}$30%. Bar = 200 µm. **[B]** Quantitative real time PCR **[qPCR]** of adherent dermal cells after chondrogenic differentiation measured on **R**elative **G**ene **E**xpression (*y* axis) among experimental groups (*x* axis). Error bars indicate mean ± standard deviation **[SD]** (*n*=3). **Black** indicates significance **p*<0.05 between positive/= $^{High-}$30% vs. negative/ $_{Low-}$30%. **Red** indicates significance **p*<0.05 against WS.

U-test). The chondrogenic potential of LAVIV® adherent dermal cells is enriched in CD271 and CD146-expressing cells.

In vitro adipogenic profile

LAVIV® adult human skin-derived dermal fractions contained cells with the ability to differentiate into adipocytes to a varying degree based on phenotype enrichment. The adipogenic potential of the adherant cells was assessed qualitatively (Figure 2A) by Oil red O staining [ORS] and quantitatively (Figure 4A) by the AdipoRed assay, which enables the visualization and quantification of intracellular lipid droplets generated by the adipocyte-like cells. Measurements were calibrated over the Non-differentiated Control [ND] as previously described. The visual assessment of the differentiated cultures stained for ORS, where the adipogenic differentiation is evaluated by red staining (black arrows Figure 4A) of the lipid droplet-rich cytoplasm, demonstrated adipogenic enrichment for only the CD146+ phenotype over negative phenotypic counterparts and WS. This result was verified quantitatively with the AdipoRed assay (Figure 4B). CD146+ sorting resulted in a higher, statistically significant, adipogenic enrichment-Kolmogorov-Smirnov-test when compared to the other phenotypes and fractions studied. CD271+ and High-30%-expressing triple-positive cells were more adipogenic than their negative/Low-30% counterparts but not more than WS. qPCR results (Figure 4C) [34] evaluated RGE for the following adipogenic markers: 1) kinase-dependent CCAAT/Enhancer-Binding Protein Alpha [CEBPA], which selectively promotes adipose-specific gene activation (i.e. leptin), 2) fatty acid binding protein 4 [FABP-4], a fatty acid chaperone expressed primarily in adipocytes that is responsible for Peroxisome Proliferator-Activated Receptor γ [PPARG] attenuation on mature adipocytes [1,35,36]; and 3) PPARG-2, a nuclear receptor target of anti-diabetic thiazolinedione drugs, responsible for adipocyte maturation [37]. Figure 4C indicates that CEBPA, FABP-4, and PPARG-2 RGEs were significantly greater in

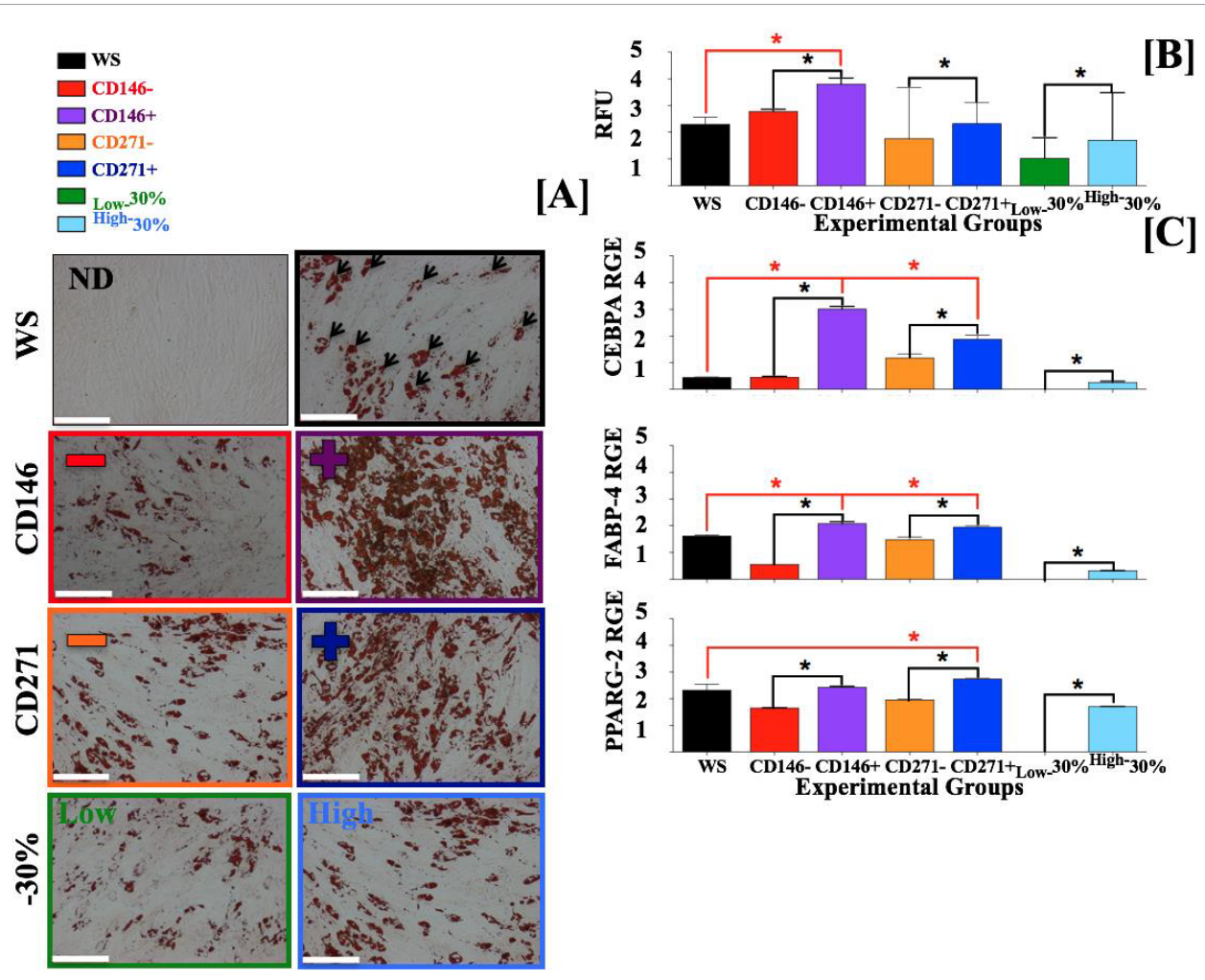

Figure 4: [A] Adherent dermal cells after adipogenic differentiation stained for Oil red where: **WS** = Mix-whole sort, **ND** = Mix-whole sort **N**ot-**D**ifferentiated control, **Arrowheads** (upper right photomicrograph) indicate intracellular lipid droplets (example), **Black** = WS, **Red** = CD146+, **Purple** = CD146-, **Orange** = CD271+, **Blue** = CD271-, **Green** = $_{Low-}$30%, **Azure** = $^{High-}$30%. Bar = 200 μm. **[B]** Quantitative AdipoRed assay of adherent dermal cells after adipogenic differentiation measured on relative fluorescence intensity [RFU] (*y* axis) among experimental groups (*x* axis). Error bars indicate mean ± standard deviation **[SD]** (*n*=6). **Black** indicates significance *p<0.05 between positive/= $^{High-}$30% vs. negative/ $_{Low-}$30%. **Red** indicates significance *p<0.05 against WS. **[C]** Quantitative real time PCR **[qPCR]** of adherent dermal cells after osteogenic differentiation measured on **R**elative **G**ene **E**xpression (*y* axis) among experimental groups (*x* axis). Error bars indicate mean ± standard deviation **[SD]** (*n*=3). **Black** indicates significance *p<0.05 between positive/= $^{High-}$30% vs. negative/ $_{Low-}$30%. **Red** indicates significance *p<0.05 against WS.

Gene	Manufacturer	Cat #	Dilution	BM-hMSC	AdSC	PHAD-10% FBS	PHAD-MSCGM
CD10	BD Pharmigen	F0826	1:50	**16%**	**24%**	**7.2%**	**>95%**
CD13	Dako	341144	1:50	93%	>95%	81%	>95%
CD29	BD Pharmigen	555443	1:50	>95%	>95%	>95%	>95%
CD34	BD Pharmigen	555824	1:100	**<1%**	**<1%**	**<1%**	**40%**
CD44	BD Pharmigen	550989	1:50	>95%	>95%	>95%	>95%
CD73	BD Pharmigen	561258	1:100	>95%	>95%	>95%	>95%
CD90	BD Pharmigen	555596	1:100	>95%	>95%	>95%	>95%
CD105	BD Pharmigen	561439	1:100	>95%	>95%	>95%	>95%
CD106	BD Pharmigen	551147	1:50	14%	<1%	<1%	<1%
CD146	ABD Serotec	MCA2141F	1:100	**>95%**	**>95%**	**40%**	**3.2%**
CD271	BD Pharmigen	560326	1:50	8%	<1%	<1%	<1%
HLA-DR	BD Pharmigen	341144	1:50	7%	<1%	<1%	<1%
NG2	eBioscience	53-6504-82	1:100	**5%**	**<1%**	**1.2%**	**6%**
SSEA-3	eBioscience	12-8833-42	1:50	5%	27%	43%	**<1%**
STRO1	SCBT	sc-47733 PerCP	1:50	<1%	<1%	<1%	<1%

Table 2: List of surface makers scrutinized including manufacturer, Cat # = catalog number and dilution utilized per 100 µL of final volume of a 1x10^6 cell suspension. BM-hMSC = Bone marrow derived-hMSC (Lonza, PT-250 Lot# 1F3284 21-years old, Hispanic female) passage # 4 (p4) cultured according the manufacturer recommendations (Lonza, 190632), AdSC = Human adipose-derived stem cells (Lonza, PT-5006 Lot# 0F4505 52 years old, Caucasian female) p4 cultured according the manufacturer recommendations (Lonza, PT-4505), PHAD cells represented by HUF-1 (human-dermal fibroblasts normal donor) 30 years old, Caucasian male accordingly obtained from Stanford University [13] at p4 -10% FBS and p5 for -MSCGM condition. Green = phenotype augment under MSCGM conditions, and Red = phenotype decrease under MSCGM. The above percentages represent the average of 3-technical replicates of over 100,000 events recorded on a FACS Fortessa cell sorter (BD Biosciences). Data were analyzed as previously described.

CD146+ and CD271+ phenotypes than in the negative phenotypes and WS but not High-30%, which solely demonstrates enrichment against the Low-30% and WS.

The adipogenic output in our cultures strongly suggested that CD146-expressing dermal derivatives are prone to form fat *in vitro* in a more efficient fashion than the remaining analyzed fractions. CD271-expressing cells denoted an adipogenic molecular profile greater than WS, nevertheless the lipid content, which is a standard factor used to assess the fat-forming potential over mesenchymal-like cells, was not greater than the WS control. This may indicate insufficient differentiation or a pre-adipocyte stage with a higher PPARG content. High-30% also enhanced adipogenesis against Low-30%, thus demonstrating the usefulness of these markers in identifying adipogenic potential.

Discussion

In this study we have isolated dermal derivatives with MSC-like competence *in vitro*, which to our knowledge, has not been documented in adult dermal cells. Human dermis contains a diverse collection of cells with ratios dependent on age, site and depth of biopsy, and many other factors [1-3]. These cells *in vivo* possess a discrete and unique set of abilities and once removed from their niche, adherent cells rapidly adapt to *ex vivo* culture conditions by either maintaining or losing these properties [1,9,35]. Previous research has revealed that a subset of Primary Human Adherent Dermal Cells (PHADs) expressing Stage Specific Embryonic Antigen-3 (SSEA-3) are transcriptionally Similar to Adipocyte-Derived Stem Cells (AdSc) [9]. Human cells expressing CD146 derived from diverse sources have been shown to differentiate *in vitro* not only into osteoblasts, chondrocytes, and adipocytes [38] but also into hepatocyte-like cells [39] and smooth muscle [40]. CD271 is an epitope that was initially identified in situ in skin punch biopsies and characterized as a strong hMSC marker over adherent dermal cells [11].

Here we have identified, isolated, and characterized three progenitor subsets from adult human dermis with unique and discrete multipotent competences. Specifically, CD146+ adherent dermal cells differentiated into bone and fat, and CD271+ cells differentiated into cartilage. Adult stem cells are indistinguishable in morphology from fibroblasts, regardless of the tissue source. Moreover, the weak performance of the canonical mesenchymal markers, CD73, CD90, and CD105 (triple positive fraction), strongly suggests the soft multipotent potential of this phenotype in the adherent adult dermal derivatives. As mentioned previously, human skin punch biopsies are quick, minimally invasive and relatively painless, and provide a primary cell population from which adult dermal stem cells can be easily accessed, purified, and preserved. This process is a suitable platform to rapidly obtain a clinically relevant number of cells for applications such as gene delivery, tissue engineering, and regenerative medicine. In particular, CD146+ dermal cells should be viable for such applications.

The above data corresponded to a single adult adherent dermal cells sample of LAVIV® (azficel-T by Fibrocell Science, DR01), PIN# 1100075 obtained from a 48-year old client at passage 5 with an estimated culture duration of five weeks. To date, we have assessed the *in vitro* differentiation of a total of three PHADs, including the cells described in this study. The multipotency of PHADs varies among cell lines [1,9,11]. *Ex vivo*, the dermal derivatives undergo drastic changes allowing the proliferation of human dermal fibroblasts and loss of the dermal derivatives with multipotent abilities [3-5]. The culture conditions such as cell density, media serum content, time in culture, oxygen tension, and small-molecule(s) supplementation may ameliorate the loss of multipotency in these cultures or in contrast, may increase the capacity to differentiate into committed lineages; however, the exact mechanisms are still yet to be fully understood [6,41-44]. Fresh PHAD cultures may yield a greater differentiation rate despite phenotype purification due a higher content of adult stem cells than older cultures [5]. Single-cell based and Colony-Forming Unit cultures (CFUs) could enhance the adult dermal stem cell derivation and phenotype stabilization, though the final yield of differentiation-inducible and therapeutically useful cells may be low, thus restricting further clinical applications [45].

Cartilage-formation from hMSCs relies on the formation of high-density cultures known as "micromasses". These three-dimensional structures act to restrain the expansion of chondrogenic cultures. Additionally, the use of biomaterials such as collagen, type I scaffolds to support PHAD chondrogenesis and culture supplementation with factors like Tumor Necrosis Factor α (TNF-α) and BMP-2 may stimulate chondrogenic and long-term cell dynamics [1,31-33].

The hMSC cell surface markers expressed on PHADs appear to be conditioned in the presence of serum components in the culture media. We compared standard culture media (10%-fetal bovine serum; FBS) with chemically-defined and serum-free media (Lonza, 190632) suitable for culture of hMSCs. The selection of media modifies cell morphology, population doubling-time, membrane fragility, and the expression of certain surface markers accompanying multipotent phenotypes *ex vivo*.

Table 2 indicates the list of markers we have scrutinized on PHADs by flow cytometry: 1) the membrane metallo-endopeptidase (CD10), previously identified as a potent mesenchymal like-cell concentrator on perivascular cells [46] and fat cells derived from lipoaspirates [47], 2) the hematopoietic progenitor cell antigen CD34, widely studied due to its therapeutic potential in vasculogenesis, osteogenesis [48], and chondrogenesis [49] with debatable hepatogenic and neurogenic potential by peripheral blood and bone marrow-derived CD34-positive cells [50,51], and 3) and the Neuron-Glial 2 antigen (NG2), initially described in pericytes promoting multilineage potential [52] demonstrating an augment from 7.2%->95% for CD10, <1%-40% for CD34, and 1.2%-6% for NG2 after one week of chemically defined and serum-free media transition. The mechanism by which this condition alters the cell's epigenetic regulation of the transcription of these markers is not yet known and will be later investigated. Additionally, an augment of the multipotent potential upon single phenotype selection has yet to be defined. Alternatively, SSEA-3 and CD146 significantly decrease from 43%-<1% and 40%-3.2%, respectively. The increasing number of small molecules, culture supplements, chemically-defined low-serum or serum-free media suitable for clinical grade expansion and differentiation might provide an appropriate environment for fresh PHADs to preserve plasticity and maintain or even augment the outlier of the multipotent phenotype on the cell-amalgam of a dermal biopsy.

Acknowledgments

This work was based on a research collaboration with Fibrocell Science, Inc. This work was supported by funding from the Eli and Edythe Broad Center of Regenerative Medicine and Stem Cell Research at UCLA and Fibrocell Science, Inc. The authors would like to thank Dr. Mirko Corselli, Stem Cell Scientist at BD for advice with regard to the hMSC antibody-based aspect of this study.

Author disclosure statement

J.A.B. and A.V.C. receive research funding from Fibrocell Science, Inc. J.A.B. is a scientific consultant for Fibrocell Science, Inc. J.A.B. and A.V.C. have no conflicts of interest or competing financial interests to report.

References

1. Junker JPE (2010) Adipogenic, chondrogenic and osteogenic differentiation of clonally derived human dermal fibroblasts. Cells Tissues Organs 191: 105-118. [PubMed]
2. Bianco P (2008) Mesenchymal stem cells: revisiting history, concepts, and assays. Cell stem cell 2: 313-319. [PubMed]
3. Manini I (2011) Multi-potent progenitors in freshly isolated and cultured human mesenchymal stem cells: a comparison between adipose and dermal tissue. Cell and Tissue Research 344: 85-95. [PubMed]
4. Sekiya I (2002) Expansion of human adult stem cells from bone marrow stroma: conditions that maximize the yields of early progenitors and evaluate their quality. Stem cells 20: 530-541. [PubMed]
5. Halfon S (2010) Markers distinguishing mesenchymal stem cells from fibroblasts are downregulated with passaging. Stem cells and development 20: 53-66. [PubMed]
6. Riekstina U (2008) Characterization of human skin-derived mesenchymal stem cell proliferation rate in different growth conditions. Cytotechnology 58: 153-162. [PubMed]
7. Auguello A (2010) Mesenchymal stem cells: a perspective from in vitro cultures to in vivo migration and niches. European Cells and Materials 20 121-133. [PubMed]
8. Kuroda Y (2010) Unique multipotent cells in adult human mesenchymal cell populations. Proceedings of the National Academy of Sciences 107: 8639-8643. [PubMed]
9. Vega-Crespo A (2012) Human skin cells that express stage-specific embryonic antigen 3 associate with dermal tissue regeneration. Bioresearch open Access 1: 25-33. [PubMed]
10. Vishnubalaji R (2012) In vitro differentiation of human skin-derived multipotent stromal cells into putative endothelial-like cells. BMC Developmental Biology 12: 12-27. [PubMed]
11. Vaculik C (2012) Human dermis harbors distinct mesenchymal stromal cell subsets. J Invest Dermatol 32: 563-574. [PubMed]
12. Nguyen T (2014) Dermatology procedures: skin biopsy. FP Essent 6: 24-28. [PubMed]
13. Byrne JA (2009) Enhanced generation of induced pluripotent stem cells from a subpopulation of human fibroblasts. PLoS One 4: e7118. [PubMed]
14. Awe JP (2013) Generation and characterization of transgene-free human induced pluripotent stem cells and conversion to putative clinical-grade status. Stem Cell Res Ther 4: 87-102. [PubMed]
15. Kadner A (2002) A new source for cardiovascular tissue engineering: human bone marrow stromal cells. Eur J Cardiothorac Surg 21: 1055-1060. [PubMed]
16. Zimmerlin L (2013) Mesenchymal markers on human adipose stem/progenitor cells. Cytometry A. 83: 34-140. [PubMed]
17. Corselli M (2013) Perivascular support of human hematopoietic stem/progenitor cells. Blood 121: 2891-2901. [PubMed]
18. Köllmer M (2013) Markers are shared between adipogenic and osteogenic differentiated mesenchymal stem cells. J Dev Bio Tissue Eng 5: 18-25. [PubMed]
19. Eyckmans J (2012) Adhesive and mechanical regulation of mesenchymal stem cell differentiation in human bone marrow and periosteum-derived progenitor cells. Biol Open 1: 1058-1068. [PubMed]
20. Bian L (2011) Enhanced MSC chondrogenesis following delivery of TGF-β3 from alginate microspheres within hyaluronic acid hydrogels in vitro and in vivo. Biomaterials 32: 6425-6434. [PubMed]
21. Zhang J (2012) BMP-2 mediates PGE(2) -induced reduction of proliferation and osteogenic differentiation of human tendon stem cells. J Orthop Res 30: 47-52.
22. Taura D (2009) Adipogenic differentiation of human induced pluripotent stem cells: comparison with that of human embryonic stem cells. FEBS Lett 583: 1029-1033. [PubMed]
23. Higuchi M (2013) Differentiation of human adipose-derived stem cells into fat involves reactive oxygen species and Forkhead box O1 mediated upregulation of antioxidant enzymes. Stem Cells Dev 22: 878-88. [PubMed]
24. Sridharan G (2012) Toluidine blue: A review of its chemistry and clinical utility. J Oral Maxillofac Pathol 16: 251-255. [PubMed]
25. Ijiri K (2005) A novel role for GADD45β as a mediator of *MMP-13* gene expression during chondrocyte terminal differentiation. J Biol Chem 280: 38544-38555. [PubMed]
26. Liva KJ (2001) Analysis of relative gene expression data using real-time quantitative PCR and the 2(-Delta Delta C (T)) Method. Methods 25: 402-408. [PubMed]
27. Field A (2009) Discovering statistics using SPSS. SAGE Publications Ltd California. Print.
28. Motulsky H (2004) Fitting models to biological data using linear and nonlinear regression. Oxford University Press London. Print
29. Kini U (2012) Physiology of bone formation remodeling, and metabolism. Radionuclide and Hybrid Bone Imaging. Fogelman I, Gnanasegaran G, et al. (editors). Chapter 2: 29-57.
30. Kirkham GR (2007) Genes and Proteins Involved in the Regulation of Osteogenesis. Topics in Tissue Engineering 3: 1-22.
31. Boeuf S (2008) A chondrogenic gene expression signature in mesenchymal

stem cells is a classifier of conventional central chondrosarcoma. J Pathol 216: 158-66. [PubMed]

32. Sekiya I (2002) In vitro cartilage formation by human adult stem cells from bone marrow stroma defines the sequence of cellular and molecular events during chondrogenesis. Proceedings of the National Academy of Sciences 99: 4397-4402. [PubMed]

33. Schmitt B (2006) BMP2 initiates chondrogenic lineage development of adult human mesenchymal stem cells in high-density culture. Differentiation 71: 567-577. [PubMed]

34. Ponce M (2008) Coexpression of osteogenic and adipogenic differentiation markers in selected subpopulations of primary human mesenchymal progenitor cells. J Cell Biochem 104: 1342-1355. [PubMed]

35. Jääger K (2010) Human dermal fibroblasts exhibit delayed adipogenic differentiation compared with mesenchymal stem cells. Stem cells and development 20:1327-1336. [PubMed]

36. Yu S (2003) Adipocyte-specific Gene Expression and Adipogenic Steatosis in the Mouse Liver Due to Peroxisome Proliferator-activated Receptor γ 1 (PPAR γ 1) Overexpression. J Biol Chem 278: 498-505. [PubMed]

37. Lefterova MI (2008) PPARγ and C/EBP factors orchestrate adipocyte biology via adjacent binding on a genome-wide scale. Genes Dev 22: 2941-2952. [PubMed]

38. Zannettino AC (2008) Multipotential human adipose-derived stromal stem cells exhibit a perivascular phenotype in vitro and in vivo. J Cell Physiol 214: 413-421. [PubMed]

39. Zuk P (2013) Adipose-Derived Stem Cells in Tissue Regeneration: A Review. ISRN Stem Cells 2013: 1-35.

40. Espagnolle N (2014) CD146 expression on mesenchymal stem cells is associated with their vascular smooth muscle commitment. J Cell Mol Med 18: 104-114. [PubMed]

41. Tsai CC (2012) Benefits of hypoxic culture on bone marrow multipotent stromal cells. Am J Blood Res 2: 148-159. [PubMed]

42. Keogh MB (2010) A novel collagen scaffold supports human osteogenesis-applications for bone tissue engineering. Cell Tissue Res 340: 169-77. [PubMed]

43. Tamama K (2009) Epidermal Growth Factor (EGF) Treatment on Multipotential Stromal Cells (MSCs). Possible Enhancement of Therapeutic Potential of MSC. J Biomed Biotechnol 10: 1-11.

44. Lee WC (2014) Multivariate biophysical markers predictive of mesenchymal stromal cell multipotency. Proc Natl Acad Sci U S A 111: 4409-4418. [PubMed]

45. Haniffa MA (2007) Adult human fibroblasts are potent immunoregulatory cells and functionally equivalent to mesenchymal stem cells. The Journal of Immunology 179: 1595-1604. [PubMed]

46. Medici D (2010) Conversion of vascular endothelial cells into multipotent stem-like cells. Nat Med 16: 1400-1406. [PubMed]

47. Ong WK (2014) Identification of specific cell-surface markers of adipose-derived stem cells from subcutaneous and visceral fat depots. Stem Cell Reports 2:171-179. [PubMed]

48. Matsumoto T (2006) Therapeutic potential of vasculogenesis and osteogenesis promoted by peripheral blood CD34-positive cells for functional bone healing. Am J Pathol 169: 1440-1457. [PubMed]

49. Mackay AM (2007) Chondrogenic Differentiation of Cultured Human Mesenchymal Stem Cells from Marrow. Tissue Engineering 4: 415-428. [PubMed]

50. Zheng YB (2008) Characterization and hepatogenic differentiation of mesenchymal stem cells from human amniotic fluid and human bone marrow: a comparative study. Cell Biol Int 32: 1439-1448. [PubMed]

51. Shih DT (2005) Isolation and characterization of neurogenic mesenchymal stem cells in human scalp tissue. Stem Cells 23: 1012-1020. [PubMed]

52. Dar A (2012) Multipotent vasculogenic pericytes from human pluripotent stem cells promote recovery of murine ischemic limb. Circulation 125: 87-99. [PubMed]